

Isospin violating decay $D_s^* \rightarrow D_s \pi^0$ in chiral perturbation theory

Bin Yang^{1,*}, Bo Wang^{2,†}, Lu Meng^{1,‡} and Shi-Lin Zhu^{1,2,§}

¹*School of Physics and State Key Laboratory of Nuclear Physics and Technology, Peking University, Beijing 100871, China*

²*Center of High Energy Physics, Peking University, Beijing 100871, China*

We systematically calculate the isospin violating decay, $D_s^* \rightarrow D_s \pi^0$, with the heavy meson chiral perturbation theory up to $\mathcal{O}(p^3)$ including the loop diagrams. The $\mathcal{O}(p^3)$ tree level amplitudes contain four undetermined LECs. We use two strategies to estimate them. With the nonanalytic dominance approximation, we get $\Gamma[D_s^* \rightarrow D_s \pi^0] = (3.38 \pm 0.12)$ eV. With the naturalness assumption, we give a possible range of the isospin violating decay width, $[1.11 - 6.88]$ eV. We find that the contribution of the $\mathcal{O}(p^3)$ corrections might be significant.

I. INTRODUCTION

The $D_{(s)}$ -mesons are composed of one charm quark and one light antiquark. The dynamics of $D_{(s)}$ -mesons is constrained by both the chiral symmetry in the light quark sector and the heavy quark symmetry in the heavy sector. The subtle interplay of the light and heavy degrees of freedom within the $D_{(s)}$ -mesons renders them a crucial platform to explore and understand QCD. $D_{s0}^*(2317)$ and $D_{s1}(2460)$ are two superstars in the D_s family due to their unexpected low mass. The couple-channel effect between the $DK^{(*)}$ scattering states and $c\bar{s}$ components leads to the mass deviation from the quark model prediction [1–3]. See Ref. [4] for a recent review. In addition, the charm quark mass is not very large. Thus decay behaviors of $D_{(s)}$ -mesons will provide us very important information about the heavy quark symmetry and the light quark dynamics.

The strong and radiative decays of the charmed mesons have been studied in many different models. For example, the chiral perturbation theory and heavy quark effect theory are used in Refs. [5–13]. Various quark models are employed in Refs. [14–20]. There are also lots of other theoretical methods such as vector meson dominance hypothesis [21], QCD sum rules [22–26], quark-potential models [14, 27–29], extended Nambu-Jona-Lasinio model [30, 31], the cloudy bag model [32], the constituent quark-meson model [33], lattice QCD simulations [34], and so on.

For the ground states, the mass splittings between $D_{(s)}^*$ and $D_{(s)}$ just lie above the pion mass m_π with 2 – 3 MeV. The constraint from phase space leads to the dominant pion and photon emission decay modes of $D_{(s)}^*$, i.e. $D_{(s)}^* \rightarrow D_{(s)}\gamma$ and $D_{(s)}^* \rightarrow D_{(s)}\pi$. For the charmed strange meson D_s^* , the decay modes are particularly interesting. $D_s^* \rightarrow D_s\pi^0$ is the strong decay process which violates the isospin symmetry. The double suppressions from phase space and the isospin violation make the hadron decay width tiny, at the order of several eVs. The branch ratio of this strong decay mode is $(5.8 \pm 0.7)\%$, which is much less than that of the electromagnetic decay $D_s^* \rightarrow D_s\gamma$ about $(93.5 \pm 0.7)\%$ [35]. The decay

mode challenges our physical intuition about the magnitude of strong decay.

The decay ratio of $\Gamma(D_s^{*+} \rightarrow D_s^+ + \pi^0)/\Gamma(D_s^{*+} \rightarrow D_s^+ + \gamma)$ have been measured in CLEO [36] and BaBar [37], respectively. Theoretically, this decay channel has been studied in Refs. [38–40] with the chiral symmetry and heavy quark symmetry, where only the tree level contributions are considered. The very exotic hadronic decay mode deserves more refined investigations.

The chiral perturbation theory is the effective field theory of low energy QCD, which is a systematic and model-independent framework. It is a powerful tool to analyze the physics associated with the light degrees of freedom within the $D_{(s)}$ -mesons below the typical energy scale, m_ρ . For the $D_{(s)}$ -mesons, the charm quark mass m_c is much larger than the light quark mass m_q ($q = u, d, s$), thus m_c can be integrated out at the low energy scale. The color-magnetic interaction in the QCD Hamiltonian is suppressed by $1/m_c$ and can be omitted at the leading order of the heavy quark effective theory. Thus, heavy quark is regarded as the static color source and the heavy quark spin symmetry is kept.

In Refs. [5–7, 41–44], the chiral effective theory incorporating heavy quark symmetry was constructed. In the effective theory, the chiral Lagrangian describes the low energy strong interactions between the heavy hadrons and light Goldstone bosons. Naturally, we can exploit this chiral effective theory to describe strong decay of the $D_{(s)}^* \rightarrow D_{(s)}\pi$.

In this work, we focus on the isospin violating decay $D_s^* \rightarrow D_s\pi^0$. We use the heavy meson chiral perturbation theory to investigate this process. Based on previous works, we not only calculate the leading order contribution, but also include the next-to-leading order loop diagrams and tree diagrams. The contributions of the loop diagrams manifest the complicated light quark dynamics, which generates some different structures from the leading ones. Besides, the m_π dependent analytic expressions might be useful to do the extrapolations in lattice QCD simulations.

This paper is organized as follows. In Sec. II, we give the effective Lagrangians with respect to the charmed mesons and light pseudoscalars. In Sec. III, we illustrate the Feynman diagrams of the decay $D_s^* \rightarrow D_s\pi^0$, the corresponding analytic expression of each diagram, and the numerical results, respectively. In Sec. IV, we give some discussions and conclusions.

* bin.yang@pku.edu.cn

† bo-wang@pku.edu.cn

‡ lmeng@pku.edu.cn

§ zhul@pku.edu.cn

II. EFFECTIVE LAGRANGIANS

One may use the chiral symmetry and the heavy quark symmetry to construct the Lagrangians that account for the heavy mesons and light pseudoscalars. The light pseudoscalar mesons octet are described by the field $U(x) = u^2 = e^{i\phi/f_\phi}$ with

$$\phi = \begin{pmatrix} \pi^0 + \frac{1}{\sqrt{3}}\eta & \sqrt{2}\pi^+ & \sqrt{2}K^+ \\ \sqrt{2}\pi^- & -\pi^0 + \frac{1}{\sqrt{3}}\eta & \sqrt{2}K^0 \\ \sqrt{2}K^- & \sqrt{2}K^0 & -\frac{2}{\sqrt{3}}\eta \end{pmatrix}, \quad (1)$$

and f_ϕ is the decay constants of the light pseudoscalars. Their experimental values are $f_\pi = 92.4$ MeV, $f_K = 113$ MeV and $f_\eta = 116$ MeV, respectively. The chiral connection is defined as

$$\Gamma_\mu \equiv \frac{1}{2} (u^\dagger \partial_\mu u + u \partial_\mu u^\dagger). \quad (2)$$

The leading order Lagrangian that describes the self-interaction of the octet pseudoscalars can be written as [38, 45]

$$\mathcal{L}_{\phi\phi} = \frac{f_\phi^2}{4} \text{Tr} [\partial_\mu U \partial^\mu U^\dagger] + \frac{f_\phi^2}{4} \text{Tr} [\chi U^\dagger + U \chi^\dagger], \quad (3)$$

where $\text{Tr}[\dots]$ denotes the trace in flavor space. The building block $\chi = 2B_0 m_q$ contains the light quark mass matrix m_q ,

$$m_q = \begin{pmatrix} m_u & 0 & 0 \\ 0 & m_d & 0 \\ 0 & 0 & m_s \end{pmatrix}, \quad (4)$$

and $B_0 = -\langle \bar{q}q \rangle / (3f_\phi^2)$ is a parameter related to the quark condensate. The second term in Eq. (3) embodies the chiral symmetry breaking effect, which implies the π^0 and η mixing vertex, i.e.,

$$\mathcal{L}_{\text{mixing}} = -\frac{B_0}{\sqrt{3}} (m_u - m_d) \eta \pi^0. \quad (5)$$

This equation demonstrates the origin of the isospin symmetry violation at the quark level, i.e., the tiny mass difference between u and d quarks.

The spin doublet of the anticharmed vectors \bar{D}^* and pseudoscalars \bar{D} can be expressed as the four-velocity dependent superfield \mathcal{H} in the heavy quark limit, i.e.,

$$\begin{aligned} \mathcal{H} &= [P_\alpha^* \gamma^\alpha + iP \gamma_5] \frac{(1 - \not{v})}{2}, \\ \bar{\mathcal{H}} &= \gamma_0 \mathcal{H}^\dagger \gamma_0 = \frac{1 - \not{v}}{2} [P_\alpha^{*\dagger} \gamma^\alpha + iP^\dagger \gamma_5], \end{aligned} \quad (6)$$

where $v = (1, \mathbf{0})$ is the four-velocity of the heavy mesons, and the charmed meson fields are denoted as

$$P^{(*)} = (\bar{D}^{0(*)}, D^{(*)-}, D_s^{(*)-}). \quad (7)$$

The leading order Lagrangian describing the low energy interactions of the anticharmed mesons and light pseudoscalars reads

$$\mathcal{L}_{P^* P \phi}^{(1)} = -i \langle \bar{\mathcal{H}} v \cdot \mathcal{D} \mathcal{H} \rangle - \frac{\Delta}{8} \langle \bar{\mathcal{H}} \sigma^{\mu\nu} \mathcal{H} \sigma_{\mu\nu} \rangle + g \langle \bar{\mathcal{H}} \psi \gamma_5 \mathcal{H} \rangle, \quad (8)$$

where $\mathcal{D}_\mu = \partial_\mu + \Gamma_\mu$, and $\langle \dots \rangle$ denotes the trace in spinor space. $\Delta = m_{P^*} - m_P$ is the mass splitting between \bar{D}^* and \bar{D} . $g \approx 0.59$ represents the axial coupling constant, which can be determined from the partial decay width of $D^{*+} \rightarrow D^0 \pi^+$ [13, 35] or lattice QCD [46]. u_μ is the chiral axial-vector current, which reads

$$u_\mu \equiv \frac{i}{2} (u^\dagger \partial_\mu u - u \partial_\mu u^\dagger). \quad (9)$$

In Eq. (8), the first term describes the kinetic energy of the heavy mesons. The second term comes from the $1/m_Q$ correction of the next-to-leading order color-magnetic interaction in heavy quark expansion. The third term gives the coupling vertices of $\bar{D}^* \bar{D} \pi$ and $\bar{D}^* \bar{D} \pi^*$.

Next we shall consider the contribution of the $\mathcal{O}(p^2)$ tree diagram. In order to construct such an $\mathcal{O}(p^2)$ Lagrangian to provide $D_s^* D_s \pi^0$ vertex, we need the building blocks χ_- and $\partial^\mu u_\mu$. If we use the building block χ_- , one should notice that the parity of this building block is negative, i.e., we have to multiply another $\mathcal{O}(p^0)$ building block with negative parity to make sure the parity of the Lagrangian is positive. However, there does not exist such a building block that can satisfy both the requirement of parity conservation and Lorentz invariance. For the other building block $\partial^\mu u_\mu$, there exists the same problem. Thus, there does not exist $\mathcal{O}(p^2)$ chiral Lagrangian contributing to the isospin violating process after considering the constraint from Lorentz invariance and CPT conservation.

In our calculation, we also consider the contribution from the loop diagrams, which will be presented in latter part. According to the power counting, the chiral order of the one-loop diagrams is at least $\mathcal{O}(p^3)$. In order to absorb the divergence in the loop diagrams, the $\mathcal{O}(p^3)$ tree-level Lagrangian is constructed as follows,

$$\begin{aligned} \mathcal{L}_{P^* P \phi}^{(3)} &= \frac{b_1}{\Lambda_\chi^2} \langle \bar{\mathcal{H}} \psi \hat{\chi}_+ \gamma_5 \mathcal{H} \rangle + \frac{b_2}{\Lambda_\chi^2} \langle \bar{\mathcal{H}} \psi \gamma_5 \mathcal{H} \rangle \text{Tr} [\chi_+] \\ &+ i \frac{c_1}{\Lambda_\chi^2} \langle \bar{\mathcal{H}} \not{\partial} \hat{\chi}_- \gamma_5 \mathcal{H} \rangle + \frac{d}{\Lambda_\chi^2} \langle \bar{\mathcal{H}} \not{\partial}_\nu \not{\partial} u^\nu \gamma_5 \mathcal{H} \rangle \\ &+ i \frac{c_2}{\Lambda_\chi^2} \langle \bar{\mathcal{H}} \gamma^\mu \gamma_5 \mathcal{H} \rangle \partial_\mu \text{Tr} [\chi_-], \end{aligned} \quad (10)$$

where $\Lambda_\chi = 4\pi f_\pi$. b_1, b_2, c_1, c_2 and d are five low energy constants (LECs). The spurions χ_\pm are introduced as

$$\chi_\pm = u^\dagger \chi u^\dagger \pm u \chi^\dagger u, \quad \hat{\chi}_\pm = \chi_\pm - \frac{1}{3} \text{Tr} [\chi_\pm]. \quad (11)$$

The Lagrangian (10) contains all possible relevant terms satisfying the requirement of the symmetries. However, the structures of the terms $\langle \bar{\mathcal{H}} \psi \gamma_5 \mathcal{H} \rangle \text{Tr} [\chi_+]$ and $\langle \bar{\mathcal{H}} \gamma^\mu \gamma_5 \mathcal{H} \rangle \partial_\mu \text{Tr} [\chi_-]$ are the same as the ones from the leading order Lagrangian. Thus they can be absorbed into Eq. (8) by renormalizing the axial coupling g . The term

$\langle \bar{\mathcal{H}} \partial_\nu \partial^\nu u_\mu \gamma^\mu \gamma_5 \mathcal{H} \rangle$ is actually the same as the fourth term in the Lagrangian in our calculation, and we did not write it in Eq. (10). With the above Lagrangians, we can analytically calculate the decay process $D_s^* \rightarrow D_s \pi^0$ up to $\mathcal{O}(p^3)$.

III. ISOSPIN VIOLATING DECAY

A. Power counting and Feynman diagrams

In chiral perturbation theory, one can use the power counting to assess the importance of Feynman diagrams generated by the effective Lagrangians when calculating the physical matrix element. The standard power counting for this process yields,

$$\mathcal{O} = 4N_L - 2I_M - I_H + \sum_n nN_n, \quad (12)$$

where N_L , I_M and I_H are the numbers of loops, internal light pseudoscalar lines and internal heavy meson lines, respectively. N_n is the number of vertices which are governed by the n -th order Lagrangians. Thus, we can write down the decay amplitude as the following expression,

$$\mathcal{M} = \mathcal{M}_{\text{tree}}^{(1)} + \mathcal{M}_{\text{tree}}^{(3)} + \mathcal{M}_{\text{loop}}^{(3)}, \quad (13)$$

where the superscripts in the parentheses represent the chiral order.



FIG. 1. The tree diagram for the $D_s^* \rightarrow D_s \pi^0$ decay at the leading order. The thick solid, thin solid and dashed lines represent the heavy vector meson D_s^* , heavy pseudoscalar meson D_s , and light pseudoscalar mesons, respectively. The solid dot denotes the $\mathcal{O}(p)$ $D_s^* D_s \eta$ vertex, and the cross represents the $\eta - \pi$ mixing vertex.

For the $\mathcal{O}(p)$ tree diagram, the isospin violating effect comes from the $\pi - \eta$ mixing as shown in Fig. 1. From Eq. (5), the $\pi - \eta$ mixing effect comes from the mass difference between u and d quarks.

The loop diagrams with the vertices from the leading order Lagrangians [e.g., see Eqs. (3), (8) and (10)] are shown in Fig. 2, which are $\mathcal{O}(p^3)$ diagrams according to the power counting law. The loop diagrams (k) and (l , m) are the renormalization of the D_s and D_s^* wave functions, respectively.

The vertex with two heavy mesons and one light pseudoscalar comes from the third term of the $\mathcal{O}(p)$ Lagrangian (8). The vertex denoted with the cross is from the Lagrangian (5). The vertex in the diagram (e , f) connecting two heavy mesons and three pseudoscalars also stems from the third term of Eq. (8), where we need to expand the axial-vector field u_μ to the second order. For the vertices with two heavy mesons and two light pseudoscalars in diagram (g , h , i , j), we can derive them in the first term of Eq. (8). The chiral

connection in the covariant derivative generates this kind of vertex.

For the $\mathcal{O}(p^3)$ loop diagrams, the isospin violating effect comes from two processes. The graphs (b , d , f , h , j) contain the $\eta - \pi$ mixing vertex which resembles the $\mathcal{O}(p)$ tree diagram. For the second type of the loop diagrams (a , c , e , g , i), they do not have the direct isospin violating vertex, i.e., $\eta - \pi$ mixing. The second type of isospin violation arises from incomplete cancellation of diagrams considering the mass splitting of particles within the same isospin multiplet in the loops. For example, we shall consider the internal light pseudoscalars such as K^- and \bar{K}^0 , when calculating the loop diagram (a). If we ignore the mass splitting between K^- and \bar{K}^0 , their contributions are exactly the same but with opposite sign. The graph (a) becomes nonvanishing and gives the isospin violating effect when the tiny mass difference $\delta_{m_K} = m_{\bar{K}^0} - m_{K^-}$ is kept. Actually, both types of isospin violating effects originate from the mass difference between the u and d quarks.

Besides the mass splitting between u and d quarks, another source of the isospin violating effect stems from the electromagnetic interaction, the charge difference between u and d quarks. The Feynman diagram is shown in Fig. 3. The vertex $\pi^0 \rightarrow 2\gamma$ denoted by the solid triangle arises from the axial-vector current anomaly. However, the Feynman amplitude of such a diagram is proportional to α^2 , where α is the fine structure constant. The contribution of this diagram is highly suppressed. Thus, it is reasonable to neglect the isospin violation from the electromagnetic interaction in our calculation.

The tree diagrams with the vertices coming from the next-to-leading order Lagrangian (10) are also $\mathcal{O}(p^3)$. We show the diagrams in Fig. 4. The $\mathcal{O}(p^3)$ tree diagram can contain the $D_s^* D_s \pi^0$ vertex, which is different from the $\mathcal{O}(p)$ one.

B. Analytical results

Using Eqs. (8) and Eq. (5), one can easily get the amplitude of the $\mathcal{O}(p)$ tree diagram [see Fig. 1], which yields

$$i\mathcal{M}^{(1)} = -\frac{g}{f_\eta} (q \cdot \varepsilon) \frac{2}{3} \frac{m_{K^0}^2 - m_{K^+}^2}{m_\eta^2 - m_\pi^2}, \quad (14)$$

where q and ε are the momentum of π^0 and polarization vector of D_s^* , respectively. The parameter $B_0(m_d - m_u)$ in Eq. (5) has been replaced by $m_{K^0}^2 - m_{K^+}^2$.

The decay amplitudes of the $\mathcal{O}(p^3)$ loop diagrams in Fig. 2 are given as follows,

$$i\mathcal{M}_{(a)}^{(3)} = \frac{g^3}{2f_K^2 f_\pi} (q \cdot \varepsilon) \left[-\frac{F(m_{K^+}, \omega_1, \delta_1)}{q_0 + \Delta_1} + \frac{F(m_{K^0}, \omega_2, \delta_2)}{q_0 + \Delta_2} \right], \quad (15)$$

$$i\mathcal{M}_{(b)}^{(3)} = \frac{g^3}{3f_\eta} (q \cdot \varepsilon) \frac{m_{K^0}^2 - m_{K^+}^2}{m_\pi^2 - m_\eta^2} \left[\frac{1}{2f_K^2} \frac{F(m_{K^+}, \omega_1, \delta_1)}{q_0 + \Delta_1} \right]$$

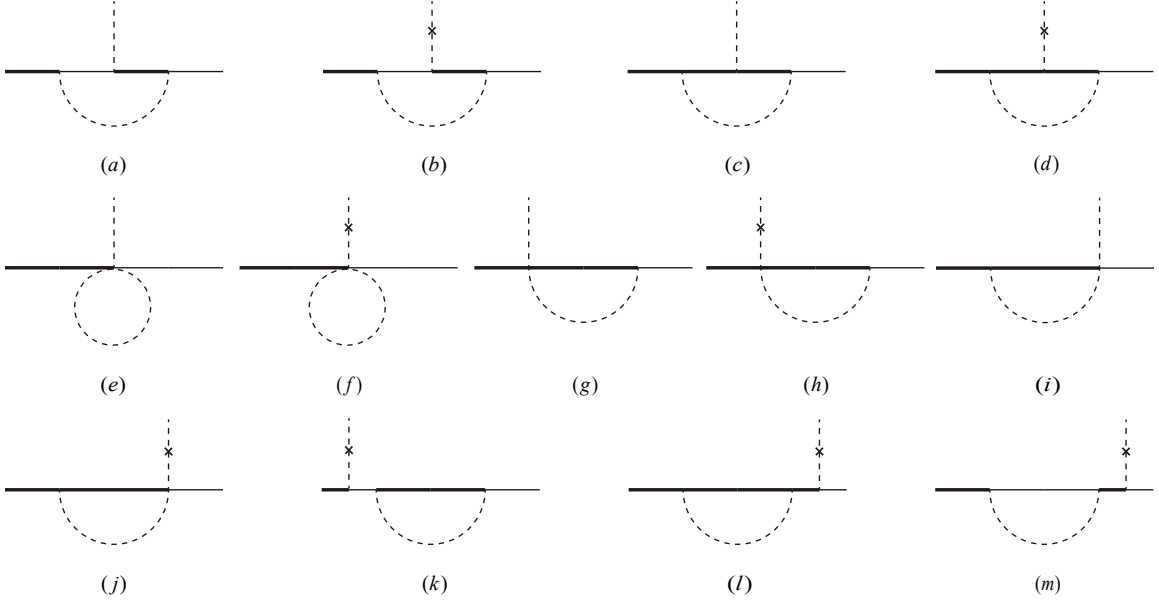


FIG. 2. The loop diagrams for the $D_s^* \rightarrow D_s \pi^0$ decay at the next-to-leading order. The notations are the same as those in Fig. 1.

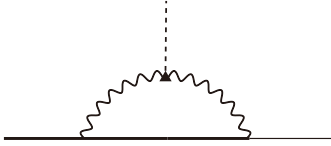


FIG. 3. A diagrammatic presentation of the axial-vector current anomaly contribution to the $D_s^* \rightarrow D_s \pi^0$ decay at the loop level. The wiggly line represents the photon, and the solid triangle denotes the $\pi^0 \gamma \gamma$ coupling vertex. Other notations are the same as those in Fig. 1.

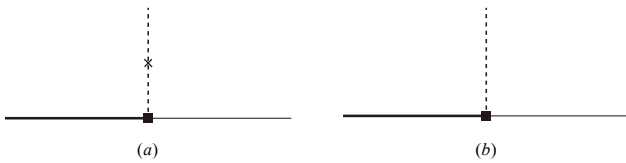


FIG. 4. The tree diagrams for the $D_s^* \rightarrow D_s \pi^0$ decay at the next-to-leading order. The solid square stands for the $\mathcal{O}(p^3)$ coupling. Other notations are the same as those in Fig. 1.

$$+ \frac{1}{2f_K^2} \frac{F(m_{K^0}, \omega_2, \delta_2)}{q_0 + \Delta_2} - \frac{2}{3f_\eta^2} \frac{F(m_\eta, \omega_3, \delta_3)}{q_0 + \Delta_3} \Big], \quad (16)$$

$$i\mathcal{M}_{(c)}^{(3)} = \frac{g^3}{f_K^2 f_\pi} (q \cdot \varepsilon) \left[\frac{F(m_{K^+}, \omega_1 - \Delta_1, \delta_1)}{q_0} - \frac{F(m_{K^0}, \omega_2 - \Delta_2, \delta_2)}{q_0} \right], \quad (17)$$

$$i\mathcal{M}_{(d)}^{(3)} = \frac{g^3(q \cdot \varepsilon)}{3f_\eta} \frac{m_{K^0}^2 - m_{K^+}^2}{m_\pi^2 - m_\eta^2} \left[\frac{F(m_{K^+}, \omega_1 - \Delta_1, \delta_1)}{-q_0 f_K^2} - \frac{F(m_{K^0}, \omega_2 - \Delta_2, \delta_2)}{q_0 f_K^2} + \frac{4}{3} \frac{F(m_\eta, \omega_3 - \Delta_3, \delta_3)}{q_0 f_\eta^2} \right], \quad (18)$$

$$i\mathcal{M}_{(e)}^{(3)} = \frac{g}{6f_K^2 f_\pi} (q \cdot \varepsilon) [J_0^c(m_{K^+}) - J_0^c(m_{K^0})], \quad (19)$$

$$i\mathcal{M}_{(f)}^{(3)} = \frac{g(q \cdot \varepsilon)}{6f_K^2 f_\eta} \frac{m_{K^+}^2 - m_{K^0}^2}{m_\pi^2 - m_\eta^2} [J_0^c(m_{K^0}) + J_0^c(m_{K^+})], \quad (20)$$

$$i\mathcal{M}_{(g)}^{(3)} = i\mathcal{M}_{(h)}^{(3)} = i\mathcal{M}_{(i)}^{(3)} = i\mathcal{M}_{(j)}^{(3)} = 0. \quad (21)$$

For the renormalization of the wave functions of the D_s meson,

$$i\mathcal{M}_{(k)}^{(3)} = i\mathcal{M}^{(1)} \delta Z_{D_s}, \quad (22)$$

where

$$\delta Z_{D_s} = Z_{D_s} - 1 = \frac{1}{2} \frac{\partial \Sigma_{D_s}(m_\phi, \omega)}{\partial \omega} \Big|_{\omega = -\Delta_3}. \quad (23)$$

And for the renormalization of the wave functions of the D_s^* meson,

$$i\mathcal{M}_{(l+m)}^{(3)} = i\mathcal{M}^{(1)} \delta Z_{D_s^*}, \quad (24)$$

where

$$\delta Z_{D_s^*} = Z_{D_s^*} - 1 = -\frac{1}{2} \frac{\partial \Sigma_{D_s^*}(m_\phi, \omega, \delta)}{\partial \omega} \Big|_{\delta=0}^{\omega=\Delta_3}. \quad (25)$$

In Eqs. (23) and (25), the expressions of Σ_{D_s} and $\Sigma_{D_s^*}$ read,

$$\Sigma_{D_s} = (1-d)g^2 \left[\frac{2}{f_K^2} J_{22}^a(m_K, \omega) + \frac{2}{3f_\eta^2} J_{22}^a(m_\eta, \omega) \right],$$

$$\Sigma_{D_s^*} = \frac{2g^2}{f_K^2} J_{22}^A(m_K, \omega, \delta) + \frac{2g^2}{3f_\eta^2} J_{22}^A(m_\eta, \omega, \delta), \quad (26)$$

where the functions $F(m, \omega, \delta)$, $J_c^0(m)$, and $J_{22}^a(m, \omega)$ are the loop integrals, which are calculated with the dimensional regularization in d dimensions. Their definitions and expressions are collected in the Appendix A. J_{22}^A is defined as

$$J_{22}^A(m, \omega, \delta) = J_{22}^a(m, \omega) + 2J_{22}^a(m, \delta). \quad (27)$$

The parameters $\omega_{1,2,3}$, $\delta_{1,2,3}$ and $\Delta_{1,2,3}$ given as,

$$\omega_1 = E - m_{D^0}, \quad \omega_2 = E - m_{D^-},$$

$$\omega_3 = E - m_{D_s}, \quad (28)$$

$$\delta_1 = E - q_0 - m_{D^{0*}}, \quad \delta_2 = E - q_0 - m_{D^{*-}},$$

$$\delta_3 = E - q_0 - m_{D_s^*}, \quad (29)$$

$$\Delta_1 = m_{D^{*0}} - m_{D^0}, \quad \Delta_2 = m_{D^{*-}} - m_{D^-},$$

$$\Delta_3 = m_{D_s^*} - m_{D_s}, \quad (30)$$

where E is the energy of D_s^* , which equals to $m_{D_s^*}$ in the center of mass frame of the initial state.

For the $\mathcal{O}(p^3)$ tree diagrams in Fig. 4, their amplitudes read,

$$i\mathcal{M}_{\text{tree}}^{(3)} = i\mathcal{M}_{(a1)} + i\mathcal{M}_{(a2)} + i\mathcal{M}_{(b)}, \quad (31)$$

with

$$i\mathcal{M}_{(a1)} = i\mathcal{M}^{(1)} \frac{1}{g\Lambda_\chi^2} \left[2(b_1 - 2c_1)m_\eta^2 - (2b_1 + d_1)m_\pi^2 \right],$$

$$i\mathcal{M}_{(a2)} = i\mathcal{M}^{(1)} \frac{1}{g\Lambda_\chi^2} \left[3(b_2 - 2c_2)m_\eta^2 + 3(b_2 + 2c_2)m_\pi^2 \right],$$

$$i\mathcal{M}_{(b)} = i\mathcal{M}^{(1)} \frac{1}{g\Lambda_\chi^2} (4c_1 - 6c_2)(m_\eta^2 - m_\pi^2), \quad (32)$$

where $\mathcal{M}^{(1)}$ is the $\mathcal{O}(p)$ amplitude in Eq. (14). The contribution of the first $\mathcal{O}(p^3)$ tree diagram contains two parts, $i\mathcal{M}_{(a1)}$ and $i\mathcal{M}_{(a2)}$. The second part can be absorbed into the leading order diagram, because they have the same Lorentz structure except a constant factor. We ignore the isospin breaking effect from the decay constants of the light pseudoscalar mesons when calculating the contribution of the loop diagrams. Because the isospin breaking effect from the K meson decay constant is about 0.1% [35, 47, 48].

After performing the average over the initial D_s^* polarization, the decay width of $D_s^* \rightarrow D_s \pi^0$ can then be written as

$$\Gamma[D_s^* \rightarrow D_s \pi^0] = \frac{|\mathbf{q}|^3}{24\pi} \frac{m_{D_s}}{m_{D_s^*}} |\mathcal{M}|^2. \quad (33)$$

C. Numerical results

We have derived the analytical expressions of the isospin violating decay $D_s^* \rightarrow D_s \pi^0$ with the chiral perturbation theory

up to $\mathcal{O}(p^3)$. However, the $\mathcal{O}(p^3)$ Lagrangian [see Eq. (10)] contains unknown LECs, which are hard to be determined at present. In order to include the effects of the $\mathcal{O}(p^3)$ tree diagrams, we use two different strategies to estimate their contributions.

Strategy A: We first adopt the nonanalytic dominance approximation [49–51] to estimate the $\mathcal{O}(p^3)$ tree diagram contributions. We know that in the chiral perturbation theory, the amplitude of a tree diagram is the polynomials of m_ϕ^2 and q^2 , i.e., it only contains the analytic terms. While for a loop diagram, its amplitude might not only contain the polynomials of m_ϕ^2 and q^2 , but also have the typical multivalued functions, such as logarithmic and square root terms, which are called as the nonanalytic terms. The nonanalytic dominance approximation assumes that the analytic part of $\mathcal{O}(p^3)$ loop diagrams and the $\mathcal{O}(p^3)$ tree diagrams are roughly the same. This approximation might be rough to some extent, but can give us some clear indications about the convergence of the chiral expansion.

We then use this strategy to estimate the $\mathcal{O}(p^3)$ tree level contribution and treat it as the error of our numerical result. Our calculation yields

$$\Gamma[D_s^* \rightarrow D_s \pi^0] = (3.38 \pm 0.12) \text{ eV}. \quad (34)$$

Considering the $\Gamma[D_s^* \rightarrow D_s \pi^0]/\Gamma[D_s^*] = (5.8 \pm 0.7)\%$, we can estimate the total width of D_s^* with the value in Eq. (34),

$$\Gamma[D_s^*] = 58.26_{-8.11}^{+10.37} \text{ eV}. \quad (35)$$

The contributions are listed in Table I order by order. The results are given in the cases of $\Delta \neq 0$ and $\Delta = 0$, respectively, where $\Delta = m_{D_{(s)}^*} - m_{D_{(s)}}$. For example, for the case of $\Delta \neq 0$, we keep all the physical mass splittings in the loops. While for the case of $\Delta = 0$, i.e., in the heavy quark limit, we neglect the mass difference of $D_{(s)}^*$ and $D_{(s)}$.

From Table I, we see that the variation of the total decay width of $D_s^* \rightarrow D_s \pi^0$ is not obvious, whereas the change of contribution from the $\mathcal{O}(p^3)$ loop diagrams is dramatic with $\Delta \neq 0$ and $\Delta = 0$. In other words, the heavy quark symmetry breaking effect at the loop level is very significant for the charm sectors. This effect has been noticed by some previous works [13, 52]. Additionally, we give the contributions of each $\mathcal{O}(p^3)$ loop diagram in Table II. We also notice that the convergence of the chiral expansion is very good, even if we work in the SU(3) case. The convergence of the $\Delta \neq 0$ case is much better than that of the $\Delta = 0$ case. In Eqs. (34) and (35) we adopt the $\Delta \neq 0$ result to predict the decay width and total width of D_s^* .

Strategy B: We consider the naturalness of the chiral perturbation theory [53, 54]. The amplitude can be expanded generally in power series of q/Λ_χ as follows,

$$\mathcal{M} = \mathcal{M}^{(0)} \sum_{\mu} \left(\frac{q}{\Lambda_\chi} \right)^{\mu} \mathcal{F}(g_i), \quad (36)$$

where $\mathcal{M}^{(0)}$ is the leading order amplitude, μ is the chiral order, and $\mathcal{F}(g_i)$ is a function of LECs. Therefore, in order to keep the convergence of the chiral expansion, a natural

TABLE I. The contributions order by order and the decay width of $D_s^* \rightarrow D_s \pi^0$ with $\Delta \neq 0$ and $\Delta = 0$, respectively. We give the numerical results of the structure $i\mathcal{M}/(q \cdot \epsilon)$ in unit of 10^{-3}GeV^{-1} , and the decay width in unit of eV.

Mass splitting	$\mathcal{O}(p)$	$\mathcal{O}(p^3)_{\text{loop}}$	$\mathcal{O}(p^3)_{\text{tree}}$	Total	$\Gamma[D_s^* \rightarrow D_s \pi^0]$
$\Delta \neq 0$	-46.90	-2.73	± 1.08	$-(49.63 \pm 1.08)$	(3.38 ± 0.12) eV
$\Delta = 0$	-46.90	-14.69	...	-61.59	5.20 eV

TABLE II. The contributions of each $\mathcal{O}(p^3)$ loop diagram with $\Delta \neq 0$ and $\Delta = 0$, respectively. We give the numerical results of the structure $i\mathcal{M}/(q \cdot \epsilon)$ in unit of 10^{-3}GeV^{-1} .

mass splitting	a	b	c	d	e	f	k	$l + m$
$\Delta \neq 0$	-1.94	-1.65	7.15	3.12	1.45	-4.86	3.03	-9.03
$\Delta = 0$	0.64	-0.25	-1.27	0.51	1.45	-4.86	4.06	-6.83

assumption requires the function $\mathcal{F}(g_i)$ should be order one. The above is the naturalness assumption of the chiral perturbation theory.

For the $\mathcal{O}(p^3)$ tree diagrams with unknown LECs, except the terms which can be absorbed by $\mathcal{O}(p^1)$ Lagrangian, we can rewrite the remaining two parts as follows,

$$i\mathcal{M}_{tree}^{(3)a1} = i\mathcal{M}^{(1)} \frac{1}{(4\pi F_\pi)^2} \alpha \left(-m_\eta^2 - \frac{3}{2} m_\pi^2 \right), \quad (37)$$

$$i\mathcal{M}_{tree}^{(3)b} = i\mathcal{M}^{(1)} \frac{1}{(4\pi F_\pi)^2} \alpha \left(-m_\eta^2 + m_\pi^2 \right). \quad (38)$$

Here we replace all the $\mathcal{O}(p^3)$ LECs as " $\alpha g/2$ ", where g is the LEC of the leading order Lagrangian, and parameter α is a order one number. The effect of the $\mathcal{O}(p^3)$ LECs can be roughly represented by the size of the parameter α . Thus, in order to discuss the contribution of the $\mathcal{O}(p^3)$ tree diagrams as much as possible, we change the parameter from -1 to 1. The change of the total decay width with the parameter is shown in Fig. 5. When the α varies from from -1 to 1, the total decay is 1.11-6.88 eV. We can see that the contribution of the $\mathcal{O}(p^3)$ tree diagrams could be quite large. Nominally, the $\mathcal{O}(p^3)$ tree diagrams should be suppressed by the factor $1/(4\pi F_\pi)^2$. But the η meson mass is 547.8 MeV, which makes the correction not as small as one naively guesses. Thus, the $\mathcal{O}(p^3)$ correction is important.

IV. SUMMARY

The heavy quark spin symmetry implies that the mass difference between the vector mesons D^* and pseudoscalar mesons D is small. Their mass splittings just lie above the pion mass with 2 – 3 MeV. Therefore, the lowest D^* mesons only have two main decay modes. One is the pion emission strong decay $D^* \rightarrow D\pi$, and the other one is the electromagnetic $D^* \rightarrow D\gamma$ decay. Generally, the decay width of

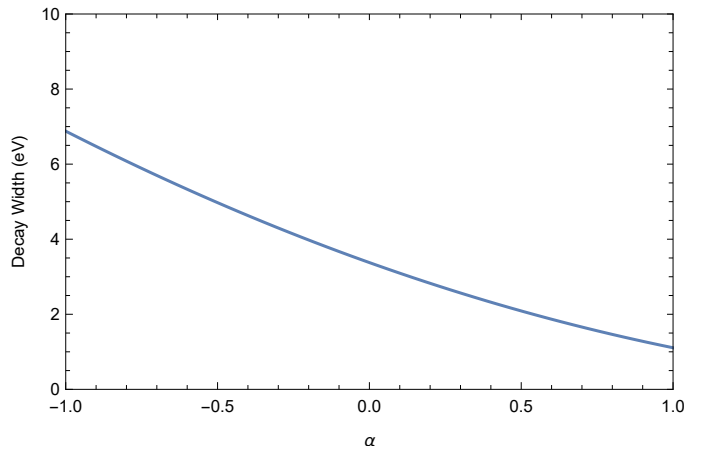


FIG. 5. The change of the decay width of $D_s^* \rightarrow D_s \pi^0$ with the parameter α .

the later one is usually much smaller than the first one due to the strength of the interactions. However, for the charmed strange meson D_s^* , the strong decay mode $D_s^* \rightarrow D_s \pi^0$ is much smaller than the electromagnetic one [35] due to the double suppression of the phase space and isospin violation.

In this work, we have systematically calculated the isospin violating decay $D_s^* \rightarrow D_s \pi^0$ with the heavy meson chiral perturbation theory up to the $\mathcal{O}(p^3)$ including the loop diagrams. The analytical expressions are derived up to chiral order $\mathcal{O}(p^3)$. For this process, the $\mathcal{O}(p^2)$ Lagrangian does not exist under constraint of the parity and Lorentz symmetries. The corrections to the leading order contribution come from the $\mathcal{O}(p^3)$ tree and loop diagrams. The vertices of the $\mathcal{O}(p^3)$ loop diagrams are governed by the leading order Lagrangians. Thus, the numerical result of the loop diagrams only depends on one parameter g , which has been well determined by experiments and lattice QCD. Our calculation of the leading order amplitude and $\mathcal{O}(p^3)$ loop diagrams shows very good convergence of the chiral expansion. The convergence in the $\Delta \neq 0$

case is much better than that in the $\Delta = 0$ one.

The $\mathcal{O}(p^3)$ tree level amplitudes contain four undetermined LECs. We use two strategies to estimate the uncertainty of the $\mathcal{O}(p^3)$ tree level contributions. With the nonanalytic dominance approximation, we get the $\Gamma[D_s^* \rightarrow D_s \pi^0] = (3.38 \pm 0.12)$ eV. With the naturalness assumption of the chiral perturbation theory, we give a possible range of the isospin violating decay width, $[1.11, 6.88]$ eV. We find that the contribution of the $\mathcal{O}(p^3)$ tree diagrams might be significant compared with the leading order one.

The isospin violating decay plays a very important role in studying the character and structure of the D_s^* meson. We expect experiments and lattice QCD can provide more results about the decays of the charmed mesons in the future. Our analytical expressions can also be helpful to the chiral extrapolations in lattice QCD simulations.

ACKNOWLEDGEMENTS

B. Yang is very grateful to W. Z. Deng, X. L. Chen for very helpful discussions. This project is supported by the National Natural Science Foundation of China under Grant 11975033.

Appendix A: Definitions and expressions of the loop integrals

The loop functions used in Eqs. (14)-(32) are defined as follows,

$$F(m_\phi, \omega, \delta) \equiv \frac{1}{d-1} \left[(m_\phi^2 - \delta^2) J_0^a(m_\phi, \delta) - (m_\phi^2 - \omega^2) \right]$$

$$J_0^a(m, \omega) = \begin{cases} -\frac{\omega}{8\pi^2} (L + \ln \frac{\lambda^2}{m^2} + 1) + \frac{1}{4\pi^2} \sqrt{\omega^2 - m^2} \operatorname{arccosh} \left(\frac{\omega}{m} \right) - \frac{i}{4\pi} \sqrt{\omega^2 - m^2} & (\omega > m) \\ -\frac{\omega}{8\pi^2} (L + \ln \frac{\lambda^2}{m^2} + 1) + \frac{1}{4\pi^2} \sqrt{m^2 - \omega^2} \operatorname{arccos} \left(-\frac{\omega}{m} \right) & (-m < \omega < m) \\ -\frac{\omega}{8\pi^2} (L + \ln \frac{\lambda^2}{m^2} + 1) - \frac{1}{4\pi^2} \sqrt{\omega^2 - m^2} \operatorname{arccosh} \left(-\frac{\omega}{m} \right) & (\omega < -m) \end{cases}. \quad (\text{A8})$$

$$\times J_0^a(m_\phi, \omega) + (\delta - \omega) J_0^c(m_\phi) \Big], \quad (\text{A1})$$

$$J_0^c(m_\phi) \equiv i \int \frac{d^d k \lambda^{4-d}}{(2\pi)^d} \frac{1}{k^2 - m_\phi^2 + i\epsilon}, \quad (\text{A2})$$

$$J_0^a(m_\phi, \omega) \equiv i \int \frac{d^d k \lambda^{4-d}}{(2\pi)^d} \frac{1}{[k^2 - m_\phi^2 + i\epsilon] [v \cdot k + \omega + i\epsilon]}, \quad (\text{A3})$$

$$\begin{aligned} & i \int \frac{d^d k \lambda^{4-d}}{(2\pi)^d} \frac{k^\mu k^\nu}{[k^2 - m_\phi^2 + i\epsilon] [v \cdot k + \omega + i\epsilon]} \\ & \equiv v^\mu v^\nu J_{21}^a(m_\phi, \omega) + g^{\mu\nu} J_{22}^a(m_\phi, \omega), \end{aligned} \quad (\text{A4})$$

The above loop integrals can be calculated with the dimensional regularization in d dimensions. Their expressions read

$$J_0^c(m) = -\frac{m^2}{16\pi^2} \left(L + \ln \frac{\lambda^2}{m^2} \right), \quad (\text{A5})$$

$$J_{22}^a(m, \omega) = \frac{1}{d-1} [(m^2 - \omega^2) J_0^a(m, \omega) + \omega J_0^c(m)]. \quad (\text{A6})$$

We adopt the $\overline{\text{MS}}$ scheme to renormalize the loop integrals. The L is defined as follows,

$$L = \frac{2}{4-d} + \ln 4\pi - \gamma_E + 1, \quad (\text{A7})$$

where $\gamma_E \approx 0.5772$ is the Euler-Mascheroni constant.

-
- [1] Y.-B. Dai, C.-S. Huang, C. Liu, and S.-L. Zhu, *Phys. Rev.* **D68**, 114011 (2003), [arXiv:hep-ph/0306274 \[hep-ph\]](#).
- [2] C. B. Lang, L. Leskovec, D. Mohler, S. Prelovsek, and R. M. Woloshyn, *Phys. Rev.* **D90**, 034510 (2014), [arXiv:1403.8103 \[hep-lat\]](#).
- [3] C. Alexandrou, J. Berlin, J. Finkenrath, T. Leontiou, and M. Wagner, (2019), [arXiv:1911.08435 \[hep-lat\]](#).
- [4] H.-X. Chen, W. Chen, X. Liu, Y.-R. Liu, and S.-L. Zhu, *Rept. Prog. Phys.* **80**, 076201 (2017), [arXiv:1609.08928 \[hep-ph\]](#).
- [5] M. B. Wise, *Phys. Rev.* **D45**, R2188 (1992).
- [6] G. Burdman and J. F. Donoghue, *Phys. Lett.* **B280**, 287 (1992).
- [7] T.-M. Yan, H.-Y. Cheng, C.-Y. Cheung, G.-L. Lin, Y. C. Lin, and H.-L. Yu, *Phys. Rev.* **D46**, 1148 (1992), [Erratum: *Phys. Rev.* **D55**, 5851 (1997)].
- [8] H.-Y. Cheng, C.-Y. Cheung, G.-L. Lin, Y. C. Lin, T.-M. Yan, and H.-L. Yu, *Phys. Rev.* **D47**, 1030 (1993), [arXiv:hep-ph/9209262 \[hep-ph\]](#).
- [9] P. L. Cho and H. Georgi, *Phys. Lett.* **B296**, 408 (1992), [Erratum: *Phys. Lett.* **B300**, 410 (1993)], [arXiv:hep-ph/9209239 \[hep-ph\]](#).
- [10] J. F. Amundson, C. G. Boyd, E. E. Jenkins, M. E. Luke, A. V. Manohar, J. L. Rosner, M. J. Savage, and M. B. Wise, *Phys. Lett.* **B296**, 415 (1992), [arXiv:hep-ph/9209241 \[hep-ph\]](#).
- [11] R. Casalbuoni, A. Deandrea, N. Di Bartolomeo, R. Gatto, F. Feruglio, and G. Nardulli, *Phys. Rept.* **281**, 145 (1997), [arXiv:hep-ph/9605342 \[hep-ph\]](#).
- [12] C.-Y. Cheung and C.-W. Hwang, *JHEP* **04**, 177 (2014), [arXiv:1401.3917 \[hep-ph\]](#).
- [13] B. Wang, B. Yang, L. Meng, and S.-L. Zhu, *Phys. Rev.* **D100**, 016019 (2019), [arXiv:1905.07742 \[hep-ph\]](#).

- [14] S. Godfrey and N. Isgur, *Phys. Rev.* **D32**, 189 (1985).
- [15] E. Sucipto and R. L. Thews, *Phys. Rev.* **D36**, 2074 (1987).
- [16] A. N. Kamal and Q. P. Xu, *Phys. Lett.* **B284**, 421 (1992).
- [17] N. Barik and P. C. Dash, *Phys. Rev.* **D49**, 299 (1994), [Erratum: *Phys. Rev.*D53,4110(1996)].
- [18] M. A. Ivanov and Yu. M. Valit, *Z. Phys.* **C67**, 633 (1995).
- [19] W. Jaus, *Phys. Rev.* **D53**, 1349 (1996), [Erratum: *Phys. Rev.*D54,5904(1996)].
- [20] H.-M. Choi, *Phys. Rev.* **D75**, 073016 (2007), [arXiv:hep-ph/0701263 \[hep-ph\]](#).
- [21] P. Colangelo, F. De Fazio, and G. Nardulli, *Phys. Lett.* **B316**, 555 (1993), [arXiv:hep-ph/9307330 \[hep-ph\]](#).
- [22] T. M. Aliev, E. Iltan, and N. K. Pak, *Phys. Lett.* **B334**, 169 (1994).
- [23] T. M. Aliev, D. A. Demir, E. Iltan, and N. K. Pak, *Phys. Rev.* **D54**, 857 (1996), [arXiv:hep-ph/9511362 \[hep-ph\]](#).
- [24] H. G. Dosch and S. Narison, *Phys. Lett.* **B368**, 163 (1996), [arXiv:hep-ph/9510212 \[hep-ph\]](#).
- [25] S.-L. Zhu, W.-Y. P. Hwang, and Z.-s. Yang, *Mod. Phys. Lett.* **A12**, 3027 (1997), [arXiv:hep-ph/9610412 \[hep-ph\]](#).
- [26] Z.-G. Wang, *Eur. Phys. J.* **C75**, 427 (2015), [arXiv:1506.01993 \[hep-ph\]](#).
- [27] J. L. Goity and W. Roberts, *Phys. Rev.* **D64**, 094007 (2001), [arXiv:hep-ph/0012314 \[hep-ph\]](#).
- [28] D. Ebert, R. N. Faustov, and V. O. Galkin, *Phys. Lett.* **B537**, 241 (2002), [arXiv:hep-ph/0204089 \[hep-ph\]](#).
- [29] V. Simonis, (2018), [arXiv:1803.01809 \[hep-ph\]](#).
- [30] H.-B. Deng, X.-L. Chen, and W.-Z. Deng, *Chin. Phys.* **C38**, 013103 (2014), [arXiv:1304.5279 \[hep-ph\]](#).
- [31] Y.-L. Luan, X.-L. Chen, and W.-Z. Deng, *Chin. Phys.* **C39**, 113103 (2015), [arXiv:1504.03799 \[hep-ph\]](#).
- [32] G. A. Miller and P. Singer, *Phys. Rev.* **D37**, 2564 (1988).
- [33] A. Deandrea, N. Di Bartolomeo, R. Gatto, G. Nardulli, and A. D. Polosa, *Phys. Rev.* **D58**, 034004 (1998), [arXiv:hep-ph/9802308 \[hep-ph\]](#).
- [34] D. Becirevic and B. Haas, *Eur. Phys. J.* **C71**, 1734 (2011), [arXiv:0903.2407 \[hep-lat\]](#).
- [35] M. Tanabashi *et al.* (Particle Data Group), *Phys. Rev.* **D98**, 030001 (2018).
- [36] J. Gronberg *et al.* (CLEO), *Phys. Rev. Lett.* **75**, 3232 (1995), [arXiv:hep-ex/9508001 \[hep-ex\]](#).
- [37] B. Aubert *et al.* (BaBar), *Phys. Rev.* **D72**, 091101 (2005), [arXiv:hep-ex/0508039 \[hep-ex\]](#).
- [38] P. L. Cho and M. B. Wise, *Phys. Rev.* **D49**, 6228 (1994), [arXiv:hep-ph/9401301 \[hep-ph\]](#).
- [39] A. N. Ivanov, (1998), [arXiv:hep-ph/9805347 \[hep-ph\]](#).
- [40] K. Terasaki, (2015), [arXiv:1511.05249 \[hep-ph\]](#).
- [41] H.-Y. Cheng, C.-Y. Cheung, G.-L. Lin, Y. C. Lin, T.-M. Yan, and H.-L. Yu, *Phys. Rev.* **D49**, 5857 (1994), [Erratum: *Phys. Rev.*D55,5851(1997)], [arXiv:hep-ph/9312304 \[hep-ph\]](#).
- [42] H.-Y. Cheng, C.-Y. Cheung, G.-L. Lin, Y. C. Lin, T.-M. Yan, and H.-L. Yu, *Phys. Rev.* **D49**, 2490 (1994), [arXiv:hep-ph/9308283 \[hep-ph\]](#).
- [43] A. N. Ivanov and N. I. Troitskaya, *Phys. Lett.* **B345**, 175 (1995).
- [44] A. N. Ivanov and N. I. Troitskaya, *Phys. Lett.* **B394**, 195 (1997).
- [45] P. L. Cho, *Phys. Lett.* **B285**, 145 (1992), [arXiv:hep-ph/9203225 \[hep-ph\]](#).
- [46] W. Detmold, C. J. D. Lin, and S. Meinel, *Phys. Rev.* **D85**, 114508 (2012), [arXiv:1203.3378 \[hep-lat\]](#).
- [47] V. Cirigliano and H. Neufeld, *Phys. Lett.* **B700**, 7 (2011), [arXiv:1102.0563 \[hep-ph\]](#).
- [48] N. Carrasco *et al.*, *Phys. Rev.* **D91**, 054507 (2015), [arXiv:1411.7908 \[hep-lat\]](#).
- [49] J. Bijnens, G. Colangelo, G. Ecker, J. Gasser, and M. E. Sainio, *Phys. Lett.* **B374**, 210 (1996), [arXiv:hep-ph/9511397 \[hep-ph\]](#).
- [50] Z.-W. Liu and S.-L. Zhu, *Phys. Rev.* **D86**, 034009 (2012), [Erratum: *Phys. Rev.*D93,no.1,019901(2016)], [arXiv:1205.0467 \[hep-ph\]](#).
- [51] B. Wang, Z.-W. Liu, and X. Liu, *Phys. Rev.* **D99**, 036007 (2019), [arXiv:1812.04457 \[hep-ph\]](#).
- [52] B. Wang, L. Meng, and S.-L. Zhu, *JHEP* **11**, 108 (2019), [arXiv:1909.13054 \[hep-ph\]](#).
- [53] E. Epelbaum, H.-W. Hammer, and U.-G. Meissner, *Rev. Mod. Phys.* **81**, 1773 (2009), [arXiv:0811.1338 \[nucl-th\]](#).
- [54] L. Meng and S.-L. Zhu, *Phys. Rev.* **D100**, 014006 (2019), [arXiv:1811.07320 \[hep-ph\]](#).